Flexoelectricity and pattern formation in nematic liquid crystals

Alexei Krekhov[*] and Werner Pesch

Physikalisches Institut, Universität Bayreuth, D-95440 Bayreuth, Germany

Ágnes Buka

Research Institute for Solid State Physics and Optics, Hungarian Academy of Sciences, H-1525 Budapest, P.O. Box 49, Hungary

We present in this paper a detailed analysis of the flexoelectric instability of a planar nematic layer in the presence of an alternating electric field (frequency ω), which leads to stripe patterns (flexodomains) in the plane of the layer. This equilibrium transition is governed by the free energy of the nematic, which describes the elasticity with respect to the orientational degrees of freedom supplemented by an electric part. Surprisingly the limit $\omega \to 0$ is highly singular. In distinct contrast to the dc case, where the patterns are stationary and time independent, they appear at finite, small ω periodically in time as sudden bursts. Flexodomains are in competition with the intensively studied electrohydrodynamic instability in nematics, which presents a nonequilibrium dissipative transition. It will be demonstrated that ω is a very convenient control parameter to tune between flexodomains and convection patterns, which are clearly distinguished by the orientation of their stripes.

I. INTRODUCTION

Nematic liquid crystals (nematics) are materials that prefer in some temperature range a uniaxial mean orientational ordering of their nonspherical molecules, while the positional order is fluidlike. The locally preferred axis is described by the director field $\boldsymbol{n}$ with $\boldsymbol{n}^2 = 1$ [1–3]. The basic equilibrium state, in the absence of external stresses, corresponds to a spatially uniform director configuration, where the orientational elastic free energy F_{el} with respect to $\boldsymbol{n}$ takes a minimum. Thus spatial variations of $\boldsymbol{n}$, which can be decomposed into splay, twist, and bend distortions with the elastic constants k_{11}, k_{22}, k_{33}, respectively, lead to an increase of F_{el}, i.e., to torques on $\boldsymbol{n}$ to restore equilibrium. In the presence of an electric field $\boldsymbol{E}$ and in nonequilibrium configurations electric torques on the director have to be considered as well. They originate from a nonzero electric polarization $\boldsymbol{P}$, which contains at first the standard dielectric contribution $\boldsymbol{P}_{\text{diel}} = \epsilon_0(\boldsymbol{\epsilon} - 1)\boldsymbol{E}$. The dielectric tensor $\boldsymbol{\epsilon}$, which depends on the local director orientation, is governed by the two dielectric permittivities $\epsilon_\parallel$ and $\epsilon_\perp$ for $\boldsymbol{E}$ parallel and perpendicular to $\boldsymbol{n}$, respectively; ϵ_0 denotes the vacuum permittivity. Furthermore, in a rough analogy to the piezo-electric polarization of certain insulators due to mechanical strains, director distortions lead also to the so-called flexopolarization, $\boldsymbol{P}_{\text{fl}} = e_1\boldsymbol{n}(\nabla \cdot \boldsymbol{n}) + e_3(\boldsymbol{n} \cdot \nabla)\boldsymbol{n}$, characterized by the two flexocoefficients e_1, e_3. If the electric field is strong enough, the balance of electric and elastic torques may even require spatially periodic director variations where typically the flexoelectric torques play a crucial role. The main goal of this paper is a detailed study of the resulting patterns, which are easily detected by optical means due to the accompanying variations of the refraction index.

Our analysis is restricted to the mostly used *planar* director configuration, which is very convenient for experimental and theoretical studies. In this case a uniform basic state is achieved by sandwiching a thin nematic layer between two plates (parallel to the x-y plane), which may also serve as electrodes for the application of a transverse electric field $\boldsymbol{E}$. By a suitable treatment of the plate surfaces the same in-plane director orientation $\boldsymbol{n} = \boldsymbol{n}_0 = \hat{\boldsymbol{x}}$ is enforced at the confining plates, which then persists throughout the whole layer in the basic state.

Before concentrating on the impact of the flexotorque we will briefly touch on the familiar consequences of the dielectric torque. It is destabilizing for a *positive* dielectric anisotropy, $\epsilon_a = \epsilon_\parallel - \epsilon_\perp > 0$, in the planar case. Thus above a certain field amplitude the compensation of the dielectric torque by the stabilizing elastic one becomes impossible and the *Freedericksz transition* takes place: The director experiences a distortion in the x–z plane, maximal at the midplane of the nematic layer [1]. The resulting director variation is in most cases uniform in the plane of the layer and varies only in the z direction. Only in some exceptional cases, when $k_{22}/k_{11} < 0.303$, the homogeneous Freedericksz transition for $\epsilon_a > 0$ is replaced by the so-called splay-twist Freedericksz transition, which leads to director distortions in the form of stripes parallel to $\boldsymbol{n}_0$. We are aware of only one experimental realization [4], since almost exclusively $0.5 < k_{22}/k_{11} < 1$ for nematics. Just for completeness, we mention that during the temporal evolution of the homogeneous Freedericksz state *transient stripe patterns* parallel to the x axis have also been described [5].

We now turn to the effect of a finite flexopolarization, which provides a robust mechanism (independent on the sign of ϵ_a) to generate stripe patterns (*flexodomains*) parallel to $\boldsymbol{n}_0$ as well. The pattern-forming instability of the basic state takes place when the flexotorque ($\propto |e_1 - e_3|$) is sufficiently strong compared with the elastic and dielectric torques [6]. Flexodomains are indeed observed in several nematic materials; also for $\epsilon_a < 0$, where a Freedericksz transition is excluded [7–9]. In this paper we present a comprehensive analysis of the flexodomains in the presence of an electric field $\boldsymbol{E} = \hat{\boldsymbol{z}}E_0 \cos(\omega t)$, both in the dc case (circular frequency $\omega = 0$) and in the ac case for small ω. Unfortunately a previous analysis of the dc case [10,11] suffers from a serious error.

————
[*]alexei.krekhov@uni-bayreuth.de

So far we have concentrated on *equilibrium transitions* driven by an electric field, which are governed by a minimization principle of the free energy. In nematics, however, we find often under the term electrohydrodynamic convection (EC) a *nonequilibrium, dissipative transition* from the basic state toward a periodic arrangement of convection rolls. Since the resulting stripes run rather perpendicular to the initial director orientation $\boldsymbol{n}_0$ they are easily distinguishable from the flexodomains. The mechanism of EC, which has been first elucidated by Carr and Helfrich [12,13] in pioneering papers, has been comprehensively discussed in a number of reviews in the last few years (see, e.g., Ref. [14] and references therein). Some new aspects of the effect of flexoelectricity on EC will be given in Sec. IV.

An interesting feature of our system is the possibility to switch between an equilibrium pattern-forming instability (flexodomains) and the dissipative EC instability just by tuning the ac frequency ω. This scenario has indeed been observed in recent experiments on certain nematics [9]: In the dc case and at very small ω one finds flexodomains, before EC takes over at increasing ω. Systematic theoretical analyzes, however, are practically missing so far. To provide those has been an important issue of our work.

In Sec. II we will briefly comment on the mathematical background of our theoretical investigations. Section III is devoted to the flexodomains. In Sec. IV we concentrate on EC at low frequencies in comparison with the transition to flexodomains. It will become obvious that in particular the limit $\omega \to 0$ is far from trivial and requires a careful analysis. The paper concludes with some final remarks.

II. MATHEMATICAL BACKGROUND

Our starting point is a nematic layer (parallel to the x-y plane) of thickness d under the action of the applied potential $U(t) = E_0 d \cos(\omega t)$ in the z direction. In the quiescent basic state the director field is homogeneous throughout the layer ($\boldsymbol{n} = \boldsymbol{n}_0 = \hat{\boldsymbol{x}}$) and flow is absent. Pattern-forming instabilities are associated with a distortion, $\delta \boldsymbol{n}$, of $\boldsymbol{n}_0$. They lead often to flow ($\boldsymbol{v} \neq 0$) and to a perturbation ϕ of the applied voltage $U(t)$. Since both the planar director orientation at $z = \pm d/2$ and $U(t)$ are considered to be fixed, the conditions $\phi = 0$ and $\delta \boldsymbol{n} = 0$ have to be fulfilled at the confining plates ($z = \pm d/2$). This applies also to $\boldsymbol{v}$ under the realistic assumption of no-slip at the boundaries.

The general theoretical framework to analyze electrically driven pattern-forming instabilities in nematic liquid crystals is well established in terms of the standard nematohydrodynamic equations [1–3]. The electric field distribution is determined by the Maxwell equations in the electroquasistatic approximation. As material parameters we need the dielectric permittivities $\epsilon_\parallel$, $\epsilon_\perp$, the electric conductivities $\sigma_\parallel$, $\sigma_\perp$ (for $\boldsymbol{n}$ parallel and perpendicular to the electric field $\boldsymbol{E}$), and the flexocoefficients e_1, e_3. The director dynamics is driven by elastic and electric torques; in the presence of flow also viscous torques have to be taken into account. The velocity field is determined by the (generalized) Navier-Stokes equation, where the viscous stress tensor depends on the orientation of $\boldsymbol{n}$ with respect to $\boldsymbol{v}$ and its gradients. For explicit calculations one needs the values of the elastic constants $k_{ii}, i = 1, 2, 3$ and furthermore

the five independent viscosity coefficients $\alpha_i, i = 1, \ldots, 5$ to quantify the stress tensor and the viscous torques. It is natural to introduce dimensionless material parameters of order one (labeled by primes). They appear then in the nondimensionalized basic equations (see, e.g., Ref. [15]) and are usually defined as follows:

$$
\begin{aligned}
k_{ii} &= k'_{ii} k_0, \quad \alpha_i = \alpha'_i \alpha_0, \\
(\sigma_\parallel, \sigma_\perp) &= (\sigma'_\parallel, \sigma'_\perp) \sigma_0, \\
(e_1, e_3) &= (e'_1, e'_3) \sqrt{\epsilon_0 k_0},
\end{aligned}
\tag{1}
$$

with

$$
k_0 = 10^{-12} \text{N}, \quad \alpha_0 = 10^{-3} \text{ Pa s}, \quad \sigma_0 = 10^{-8} (\Omega \text{ m})^{-1},
$$
$$
\epsilon_0 = 8.8542 \times 10^{-12} \frac{\text{A s}}{\text{V m}}.
\tag{2}
$$

For quantitative calculations in this paper we refer to the standard nematic N-p-methoxybenzylidene p-n-butylaniline (MBBA) [16], which has been used in many experimental investigations in the past. The material parameters of MBBA are well known; for instance, for the analysis of flexodomains we use the following dimensionless elastic and electric constants (the primes are omitted):

$$
\begin{aligned}
k_{11} &= 6.66, \quad k_{22} = 4.2, \quad e_1 = -3.25, \\
e_3 &= -4.59, \quad \epsilon_a = -0.53.
\end{aligned}
\tag{3}
$$

By using Eq. (1) it is conventional to measure lengths in units of d/π, time in units of $\tilde{\tau}$, and to introduce a dimensionless control parameter R instead of the voltage amplitude U_0, where

$$
R = \frac{\epsilon_0 E_0^2 d^2}{k_0 \pi^2} = \frac{\epsilon_0 U_0^2}{k_0 \pi^2}, \quad \tilde{\tau} = \frac{\alpha_0 d^2}{k_0 \pi^2}.
\tag{4}
$$

To describe the onset behavior of the pattern-forming instabilities the nematohydrodynamic equations are linearized about the basic state. As a result we arrive at a linear system of coupled partial differential equations in the variables x, y, z, t for the perturbations $\delta \boldsymbol{n} = (0, n_y, n_z)$, $\boldsymbol{v}$, and ϕ. Since the lateral extensions of the nematic layer are much larger than the layer thickness d, periodic boundary conditions in the layer plane are appropriate. By switching accordingly with respect to the planar coordinates $\boldsymbol{x} = (x, y)$ to Fourier space $\boldsymbol{q} = (q, p)$, one gets the linear equations in the form to be found in the Appendix of Ref. [15]; a simplified version to analyze the flexodomains will be presented explicitly in Sec. III.

As already explained, the perturbations $\delta \boldsymbol{n}, \boldsymbol{v}, \phi$ are assumed to vanish at $z = \pm d/2$; this is guaranteed by expanding these fields in terms of a complete set of Galerkin trial functions, which vanish at $z = \pm \pi/2$ in dimensionless units. For instance, the director component $n_z(\boldsymbol{q}, z, t)$ is represented as

$$
n_z(\boldsymbol{q}, z, t) = \sum_{m=1}^{M} \bar{n}_z(\boldsymbol{q}, m, t) S_m(z),
\tag{5}
$$

with $S_m(z) = \sin[m(z + \pi/2)]$. We have tested that using a truncation parameter $M = 4$ yields already data to an accuracy of better than 0.1%; in many cases even $M = 2$ is sufficient. Introducing the symbolic vector $\boldsymbol{V}(\boldsymbol{q}, t)$ for the expansion coefficients $\bar{n}_z(\boldsymbol{q}, m, t)$, $m = 1, \ldots M$ [Eq. (5)] and

the corresponding ones for n_y, $\boldsymbol{v}$, ϕ we arrive after projection onto the trial functions at a linear system of coupled ordinary differential equations of the following form:

$$\mathcal{C}(\boldsymbol{q},t)\frac{\partial}{\partial t}\boldsymbol{V}(\boldsymbol{q},t) = \mathcal{L}(R,\boldsymbol{q},t)\boldsymbol{V}(\boldsymbol{q},t). \qquad (6)$$

The matrices $\mathcal{C}$ and $\mathcal{L}$ are periodic with the ac voltage period $T = 2\pi/\omega$. The general solutions of Eq. (6) have the Floquet representation $\boldsymbol{V}(t) = \exp(\sigma t)\boldsymbol{V}_0(t)$ with $\boldsymbol{V}_0(t + T) = \boldsymbol{V}_0(t)$, where σ defines the Floquet exponent. We are interested in time-periodic solutions $\boldsymbol{V}(t)$. Here σ has to be purely imaginary of the form $\sigma = i\omega k/l$ with co-prime integers $l > k$. As a result the period of $\boldsymbol{V}(t)$ is given as lT if $k \neq 0$ and as T if $k = 0$. For a given $\boldsymbol{q}$ periodic solutions exist only for a discrete set of control parameters $R = R_0(\boldsymbol{q}) < R_1(\boldsymbol{q}) < R_2(\boldsymbol{q})$, etc. Minimizing $R_0(\boldsymbol{q})$ with respect to $\boldsymbol{q}$ yields the critical wave vector $\boldsymbol{q}_c$ and the critical control parameter $R_c = R_0(\boldsymbol{q}_c)$ at which the quiescent basic state becomes unstable. In the context of the present paper the destabilizing modes at onset had always the period T; i.e., they are characterized by $\sigma = 0$.

We have used two methods to calculate the periodic solutions of Eq. (6). One option is to expand $\boldsymbol{V}_0(t)$ into a (truncated) Fourier series in terms of $\exp(in\omega t)$ with $|n| \leqslant N$. Then Eq. (6) transforms into an algebraic linear eigenvalue problem for the Fourier coefficients, from which we obtain $R_0(\boldsymbol{q})$ (for more details see Ref. [15]). As will be documented below the time variations in $\boldsymbol{V}(t)$ become increasingly sharper with decreasing ω; consequently many Fourier modes up to $N = 60$ had to be eventually kept. Thus, in an alternative, less time-consuming approach, we construct numerically the matrix solution $\mathcal{P}(t)$ of Eq. (6) for the initial condition $\mathcal{P}(0) = \boldsymbol{I}$ where $\boldsymbol{I}$ denotes the unit matrix (see, e.g., Ref. [17] and for a recent application Ref. [18]). We have to calculate the eigenvalues $\mu_1, \mu_2, \ldots$ of the "monodromy matrix" $\boldsymbol{M} \equiv \mathcal{P}(t = T)$ where $|\mu_1| > |\mu_2|$, etc. A periodic solution of Eq. (6) with period T exists when $\mu_1 = 1$. The smallest R to fulfill this condition yields again $R = R_0(\boldsymbol{q})$.

As demonstrated in Ref. [15], the general nematohydrodynamic equations as used in this paper are invariant against a reflection $z \rightarrow -z$ at the midplane combined with a translation in time by half a period $T/2$. Thus the solution manifold of Eq. (6) naturally splits into separate classes with different parity $\mathfrak{p} = \pm 1$, for which the notions "conductive" ($\mathfrak{p} = 1$) and "dielectric" ($\mathfrak{p} = -1$), respectively, have been introduced. For instance, with respect to the director component n_z one finds $n_z(-z, t + T/2) = \mathfrak{p}\, n_z(z,t)$ (for more details, see Ref. [15]). This means that for the dielectric symmetry the time average of n_z vanishes, while it is finite for the conductive symmetry.

III. FLEXODOMAINS

In the following we will investigate the bifurcation to flexodomains, which leads to stripe patterns with the wave vector $\boldsymbol{q} = (0, p)$. It is easy to see that $U(t)$ is not modified, i.e., $\phi \equiv 0$. Inspection of the full nematohydrodynamic equations (for instance, in Ref. [15]), shows that time variations of the director at nonzero ω lead in principle to a "back flow," which acts back onto the director in the form of viscous

torques. They lead to small corrections to the dielectric and flexotorques of the order $O(\alpha_3^2/\eta_2^2)$, with the Miesowicz coefficient $\eta_2 = (\alpha_3 + \alpha_4 + \alpha_6)/2 > 0$. Since $|\alpha_3/\eta_2|^2 = O(10^{-3}$–$10^{-4})$ for MBBA and similar nematics, the viscous torques are safely neglected in this paper, which also facilitates the quasianalytical approaches in Sec. III B. Moreover, this approximation has been validated by full numerical studies of the basic equations.

It is convenient to introduce instead of the elastic constants k_{11}, k_{22} their average value k_{av}, and their relative deviation δk from k_{av} as follows:

$$k_{11} = k_{av}(1 + \delta k), \qquad k_{22} = k_{av}(1 - \delta k), \qquad (7)$$

where obviously $|\delta k| < 1$. In contrast to the rodlike nematics like MBBA where $k_{22} < k_{11}$, i.e., $\delta k > 0$ [see Eq. (3)], discotic nematics are characterized by $k_{22} > k_{11}$ ($\delta k < 0$) [19]. Thus our analysis will cover negative δk for completeness as well. Neglecting the back flow effects ($\boldsymbol{v} = 0$) the director dynamics in flexodomains is only determined by dielectric and flexotorques. We start from the linear perturbations $\delta \boldsymbol{n}(y,z,t)$ of the basic state in position space and switch to Fourier space using the (real) ansatz:

$$n_y(y,z,t) = \sin(py)\bar{n}_y(z,t), \quad n_z(y,z,t) = \cos(py)\bar{n}_z(z,t). \qquad (8)$$

As a consequence the general equations (6) reduce to the following linear system of coupled partial differential equations (PDEs) in the variables z and t for the Fourier components $\bar{n}_y$ and $\bar{n}_z$:

$$\partial_t \bar{n}_y = -[p^2(1 + \delta k) - (1 - \delta k)\partial_{zz}]\bar{n}_y \\ + p[\text{sgn}(e_1 - e_3)u\cos(\omega t) - 2\delta k\partial_z]\bar{n}_z, \qquad (9a)$$

$$\partial_t \bar{n}_z = -[p^2(1 - \delta k) - \mu u^2\cos^2(\omega t) - (1 + \delta k)\partial_{zz}]\bar{n}_z \\ + p[\text{sgn}(e_1 - e_3)u\cos(\omega t) + 2\delta k\partial_z]\bar{n}_y. \qquad (9b)$$

Instead of the time scale $\tilde{\tau}$ and the main control parameter R [Eq. (4)] we have used in Eq. (9) the director relaxation time τ_d and the dimensionless voltage amplitude u, which are defined as follows:

$$u^2 = \frac{1}{\mu}\frac{\epsilon_a}{k_{av}}R = \frac{1}{\mu}\frac{\epsilon_a}{k_{av}}\frac{\epsilon_0 E_0^2 d^2}{k_0\pi^2}, \qquad \tau_d = (\gamma_1/k_{av})\tilde{\tau}$$

$$\text{with } \mu = \frac{\epsilon_a k_{av}}{(e_1 - e_3)^2} \text{ and } \gamma_1 = \alpha_3 - \alpha_2. \qquad (10)$$

Note that we will often refer in the following to the parameter μ as a reduced measure of the dielectric anisotropy ϵ_a. Furthermore it should be realized that in Eqs. (9) and (10) only the difference of the flexocoefficients $(e_1 - e_3)$ comes into play. It is sufficient to confine oneself to the case $(e_1 - e_3) > 0$, since the solutions of Eqs. (9) for $(e_1 - e_3) \rightarrow -(e_1 - e_3)$ can be recovered by the transformation $\{\bar{n}_y(z), \bar{n}_z(z)\} \rightarrow \{\bar{n}_y(z), \bar{n}_z(-z)\}$.

A. Flexodomains driven by a dc voltage

This subsection is devoted to the analysis of the flexodomains in the dc case ($\omega = 0$) where Eqs. (9) are exact due to $\boldsymbol{v} \equiv 0$. Because all coefficients in Eqs. (9) are constant, the familiar separation ansatz $\bar{n}_{(y,z)}(z,t) = e^{\sigma t}\tilde{n}_{(y,z)}(z)$ can be used to get rid of the time dependence. Thus the time derivatives ∂_t in Eqs. (9) are replaced by σ, and one arrives at an
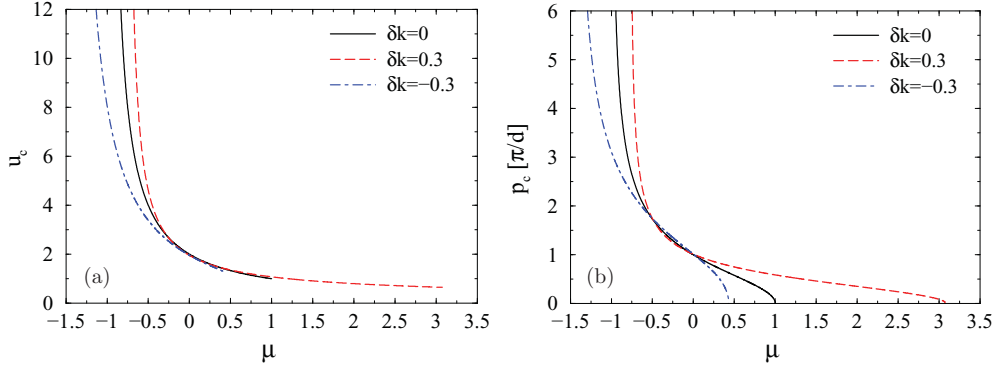
FIG. 1. (Color online) Critical voltage u_c (a) and critical wave number p_c (b) as a function of μ for $\delta k = 0$ ($\mu_{min} = -1$, $\mu_{max} = 1$), for $\delta k = 0.3$ ($\mu_{min} = -0.769$, $\mu_{max} = 3.072$), and for $\delta k = -0.3$ ($\mu_{min} = -1.427$, $\mu_{max} = 0.413$).

autonomous linear system of ordinary differential equations (ODEs) for the functions $\tilde{n}_{(y,z)}(z)$. As they have to vanish at $z = \pm\pi/2$, the eigenvalues σ will belong to a discrete set. The condition that the maximal eigenvalue $\sigma = \sigma_0(u,p)$ (growth rate) vanishes, determines the nondimensional neutral curve $u_0(p)$. The minimum of $u_0(p)$ at $p = p_c$ yields the critical voltage $u_c = u_0(p_c)$, where (u_c, p_c) depend on δk and μ. Alternatively $u_0(p)$ is given as the smallest u value, where Eqs. (9) have time-independent solutions, which vanish at $z = \pm\pi/2$. Inspection of Eqs. (9) shows that $u_0(p)$ is even in p since it depends only on p^2.

Let us first concentrate on the case of a destabilizing dielectric torque with positive ϵ_a where $\mu \propto \epsilon_a > 0$ [see Eq. (10)]. For $p = 0$ Eqs. (9) can be easily solved by choosing $\tilde{n}_y \equiv 0$ and $\tilde{n}_z \propto \sin(z + \pi/2)$. As a result we obtain

$$u_c(p=0)^2 \equiv u_F^2 = (1 + \delta k)/\mu. \tag{11}$$

This solution obviously describes the homogeneous splay Freedericksz distortion of the director. In fact, we recover from u_F^2 with the help of Eq. (10) the familiar critical Freedericksz voltage $U_0 = U_F = \pi\sqrt{k_0 k_{av}(1 + \delta k)/(\epsilon_a \epsilon_0)}$ in physical units (which is not influenced by the flexoeffect). Clearly the condition $u_0(p_c) = u_c < u_F$ is necessary for the prevalence of flexodomains with wave number $p_c \neq 0$ against the homogeneous Freedericksz distortion. It will turn out that they exist only for μ less than an upper limit $\mu_{max}(\delta k)$, at which their critical wave number p_c approaches zero.

In the case of negative ϵ_a ($\mu < 0$), on the other hand, the dielectric torque is stabilizing. It overcomes eventually the destabilizing flexotorques when μ approaches a lower limit $\mu_{min}(\delta k) < 0$ from above, where p_c diverges. Thus the director remains undistorted in the basic planar state for $\mu < \mu_{min}(\delta k)$.

In general, the z dependence of the functions $\tilde{n}_{y,z}(z)$, which have to fulfill the ODEs introduced above, is captured by an ansatz $\propto e^{\lambda z}$. In our case we obtain four different values $\lambda = \pm\lambda_1$, $\pm i\lambda_2$, where only real λ_i are compatible with the existence of flexodomains. The general solution, which consists of a linear combination of the four exponentials $e^{\pm\lambda_1 z}$, $e^{\pm i\lambda_2 z}$ has to fulfill the boundary conditions of vanishing $\tilde{n}_y$, $\tilde{n}_z$ at $z = \pm\pi/2$. As shown in the Appendix, one arrives thus at the following implicit equation for the neutral curve $u_0(p)$:

$$A_1 \sinh(\lambda_1 \pi) \sin(\lambda_2 \pi)$$
$$+ A_2 \lambda_1 \lambda_2 [1 - \cosh(\lambda_1 \pi) \cos(\lambda_2 \pi)] = 0. \tag{12}$$

For the explicit expressions of the λ_i, A_i, $i = 1,2$, which depend on p, u, δk, μ, we refer to the Appendix as well. Equation (12) represents the neutral curve $u_0(p)$ in implicit form. Minimization of $u_0(p)$ with respect to p gives the critical wave number p_c and the corresponding critical voltage $u_c \equiv u_0(p_c)$ of the flexodomains.

In Fig. 1(a) we show representative examples for u_c as a function of μ for $\delta k = 0$ and for $\delta k = \pm 0.3$ calculated with the help of Eq. (12). The corresponding critical wave numbers p_c are shown in Fig. 1(b). As discussed before the Freedericksz state with $p_c = 0$ and $u_c(0) = u_F$ is smoothly approached when $\mu \to \mu_{max}(\delta k)$. Decreasing μ from μ_{max} on is associated with a monotonic increase of both u_c and p_c until they diverge at $\mu = \mu_{min}(\delta k) < 0$. It is obvious that the knowledge of the limit curves $\mu_{min}(\delta k)$ and $\mu_{max}(\delta k)$ plays an important role to identify the regime of flexodomains in dependence on the parameters μ and δk. Thus we show these limit curves in Fig. 2 in the $(\mu, \delta k)$ plane, where $|\delta k| < 1$ according to Eq. (7). On a first look, it is surprising that $\mu_{max}(\delta k)$ diverges at $\delta k \approx 0.53$. However, as discussed in detail in the following subsection, this divergence is closely related to the existence of the (spatially periodic) splay-twist Freedericksz transition for $\delta k \gtrsim 0.53$ in the absence of the flexotorque ($e_1 - e_3 = 0$) [4].

Before we turn, however, to further discussions of Eq. (12), we present at first a very useful approximate analysis of
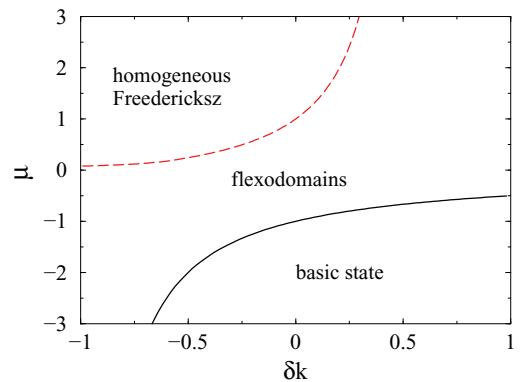

FIG. 2. (Color online) Upper and lower limit curves, $\mu_{max}(\delta k)$ (dashed, red) and $\mu_{min}(\delta k)$ (solid, black), respectively, in the $(\delta k - \mu)$ plane. $\mu_{max}(\delta k)$ diverges for $\delta k \approx 0.53$, while $\mu_{min} \to -\infty$ for $\delta k \to -1$.

flexodomains for small $|\delta k|$. Instead of using Eq. (12) directly it is more transparent to start again from Eqs. (9), by introducing the "one-mode" approximation $\tilde{n}_{(y,z)} \propto \sin(z + \pi/2)$. One obtains then immediately a quadratic equation for the eigenvalues σ; the largest one determines the growth rate σ_0. Note that in this approximation the terms $\propto 2p\delta k \partial_z \tilde{n}_{(y,z)}$ in Eqs. (9) do not contribute. Standard perturbation analysis shows that they would produce corrections of the order δk^2 to σ_0. The condition $\sigma_0 = 0$ leads within the one-mode approximation to the following expression for the neutral curve:

$$u_0^2(p) = \frac{(p^2+1)^2 - \delta k^2(p^2-1)^2}{p^2 + \mu[p^2+1+\delta k(p^2-1)]} \quad (13)$$

with its minimum at $p^2 = p_c^2$, where

$$p_c^2 = \frac{(-1+\delta k^2)\mu + \sqrt{(1+\delta k)[1+\delta k(1+4\mu)]}}{(1+\delta k)[1+\mu(1+\delta k)]}. \quad (14)$$

The explicit expression for $u_c^2 = u_0^2(p_c)$ obtained from Eqs. (13) and (14) is quite lengthy and will not be shown. According to the general remarks above, the μ interval, where flexodomains exist, can in general be read off from p_c^2 given in Eq. (14): The zero of the numerator determines the upper limit $\mu_{\max}$ and the zero of the denominator the lower limit $\mu_{\min}$. Thus we obtain the following approximate expressions valid for small δk:

$$\mu_{\min}^a(\delta k) = -\frac{1}{1+\delta k}, \quad \mu_{\max}^a(\delta k) = \frac{1+\delta k}{(1-\delta k)^2}. \quad (15)$$

The one-mode approximation becomes exact in the special case $\delta k = 0$ (one constant approximation, $k_{11} = k_{22}$), where it yields a rigorous solution of Eqs. (9). We recover in this case the results of Ref. [6]:

$$p_c^2 = \frac{1-\mu}{1+\mu}, \quad u_c^2 = \frac{4}{(1+\mu)^2}, \quad (16)$$

where $\mu_{\min}(0) = -1$ and $\mu_{\max}(0) = 1$. In general the exact neutral curve from Eq. (12) is described to an accuracy of better than 0.5% by Eq. (13) for small $|\delta k| < 0.2$. We will demonstrate below that $\mu_{\min}^a(\delta k)$ given in Eq. (15) even coincides with the exact curve $\mu_{\min}(\delta k)$ shown in Fig. 2 for all $|\delta k| < 1$.

Finally we would like to stress that our analysis of flexodomains is at variance with recent investigations [10,11] on the same subject. It will be explained in more detail in the Appendix that this work suffers from a basic mathematical error. Thus, for instance, the prediction of a "singular" behavior of p_c and u_c in both cases $k_{11}/k_{22} = 3$ ($\delta k = 1/2$) and $k_{11}/k_{22} = 1/3$ ($\delta k = -1/2$) is unfounded.

1. Analytical treatment of $\mu_{max}(\delta k)$ and $\mu_{min}(\delta k)$

So far we have given the exact description of flexodomains through Eq. (12). In addition we have demonstrated the usefulness of the analytical one-mode approximation (13) of the neutral curve $u_0(p)$ at small δk. In this section we will derive analytical expressions for the limiting curves $\mu_{\min}(\delta k)$ and $\mu_{\max}(\delta k)$ in the whole range $-1 < \delta k < 1$.

Let us start with the discussion of $\mu_{\max}(\delta k)$ for the case $\mu > 0$, where we have competition between the flexodomains and the homogeneous Freedericksz state. In Fig. 3 we show
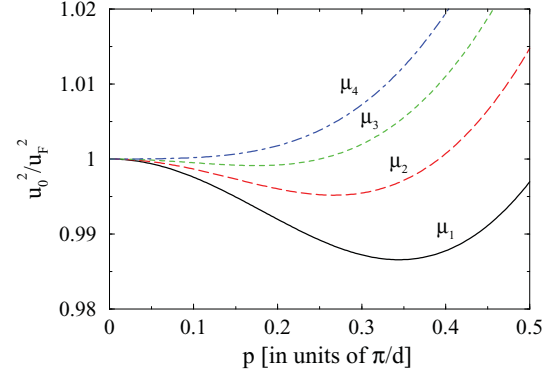

FIG. 3. (Color online) The neutral curve $u_0^2(p)$ normalized to the Freedericksz threshold u_F Eq. (11) as a function of p for $\delta k = 0.2$ and different μ with $\mu_1 = 1.4, \mu_2 = 1.6, \mu_3 = 1.8, \mu_4 = 2.0$.

a typical neutral curve $u_0(p)$ for $\delta k = 0.2$ and different μ obtained from Eq. (12). At $p = 0$ the function $u_0(p)$ has an extremum with $u_0(0) = u_F$; see Eq. (11). For $\mu < \mu_{\max}(\delta k)$ this point corresponds to a maximum where $\partial_p^2 u_0(p = 0) < 0$; here and in the following the notation ∂_p^n for the derivatives (d^n/dp^n) has been used. The minimum of $u_0(p)$ at finite $p = p_c$ where $\partial_p^2 u_0(p = p_c) > 0$ and $u_0(p_c) = u_c < u_F$ describes the flexodomains with wave number $p = p_c$.

With increasing μ both the critical wave number p_c and the difference $(u_F - u_c)$ decrease in Fig. 3. At $\mu = \mu_{\max}(\delta k) = 1.965$ the minimum and the maximum of $u_0(p)$ merge at $p = 0$. Thus the equations $u_0(p = 0) = u_F$ and $\partial_p^2 u_0(p = 0) = 0$ are fulfilled, which can be solved with respect to μ by expanding Eq. (12) up to order $O(p^2)$. The resulting analytical solution is given as $\mu = \overline{\mu}_{\max}(\delta k)$ with

$$\overline{\mu}_{\max}(\delta k) = \frac{1+\delta k}{1 - 2\delta k + \delta k^2(32/\pi^2 - 3)}. \quad (17)$$

It is convenient to introduce also the function $\delta k_F(\mu)$ as the inverse of $\overline{\mu}_{\max}(\delta k)$, which is given as

$$\delta k_F(\mu) = \frac{1 + 2\mu - \sqrt{(4\mu-1)^2 - 128\mu(\mu-1)/\pi^2}}{2\mu(32/\pi^2 - 3)}. \quad (18)$$

Thus $\delta k_F(\mu)$ marks at fixed μ the transition from the homogeneous Freedericksz state for $\delta k < \delta k_F(\mu)$ to the flexodomains in the interval $\delta k_F(\mu) < \delta k < 1$ (see also Fig. 2). The special case $\delta k_F(\mu = 1) = 0$ is consistent with $\mu_{\max}(0) = 1$ [see Eqs. (16)].

From our reasoning it seems obvious that the analytical expression $\overline{\mu}_{\max}(\delta k)$ should reproduce the curve $\mu_{\max}(\delta k)$ shown in Fig. 2. As demonstrated in Fig. 4 this is indeed the case for the interval $-\delta k_{\mathrm{low}} < \delta k < 1$ where $\delta k_{\mathrm{low}} \approx -0.566$. On this δk interval we will first concentrate.

One sees immediately that the denominator of $\overline{\mu}_{\max}(\delta k)$ approaches zero (i.e., $\overline{\mu}_{\max}$ diverges) when δk approaches a critical value $\delta k_c > 0$ from below, where δk_c is given as

$$\delta k_c = \frac{1 - 2\sqrt{1 - 8/\pi^2}}{32/\pi^2 - 3} = 0.5346. \quad (19)$$

Consistently $\delta k_F(\mu)$ in Eq. (18) approaches for $\mu \to \infty$ the limit δk_c. As a result, flexodomains exist for any $\mu > 0$ when
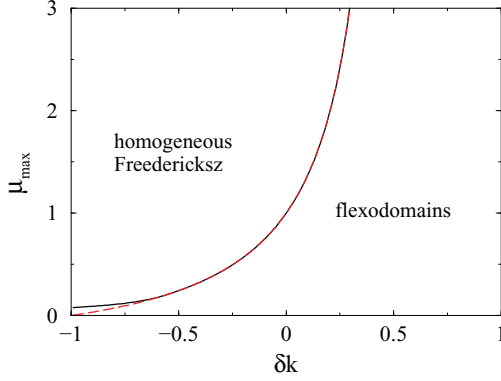
FIG. 4. (Color online) Upper limit curve $\mu_{\max}$ (solid line, black) as a function δk from Eq. (12) in comparison with $\overline{\mu}_{\max}$ from Eq. (17) (dashed line, red).

FIG. 5. (Color online) Relative critical voltage u_c^2/u_F^2 and the critical wave number p_c as function of δk for $\mu = 2$ (solid line for u_c^2/u_F^2 and dotted line for p_c, black) and in the absence of the flexoeffect ($e_1 - e_3 = 0$) (dashed line for u_c^2/u_F^2 and dot-dashed line for p_c, red). For $\mu = 2$ the Freedericksz state is approached at $\delta k_F \approx 0.206$, while this happens for $e_1 - e_3 = 0$ at $\delta k = \delta k_{\mathrm{ST}}$ [data from Eq. (12)].

$\delta k > \delta k_c$, while they are restricted to the region $\mu < \overline{\mu}_{\max}(\delta k)$ in the case of $\delta k < \delta k_c$.

It is not a coincidence that δk_c is very near to the number $\delta k_{\mathrm{ST}} \approx 0.53$, which has been quoted in the literature more than two decades ago in a different context: According to [4] the homogeneous Freedericksz transition, in the *absence of flexoeffects* ($e_1 - e_3 = 0$), is replaced for $\delta k > \delta k_{\mathrm{ST}}$ by the spatially periodic splay-twist (ST) Freedericksz transition. Similar to the flexodomains a state of finite n_y, n_z bifurcates from the basic state, which is periodic in the y direction with a critical wave number p_c, to balance the dielectric and the elastic torques. In this case additional flexotorques should not play a crucial role and the striped director configuration should develop even at arbitrary small $|e_1 - e_3|$, which corresponds to an arbitrary large $\mu = \epsilon_a k_{\mathrm{av}}/(e_1 - e_3)^2$. In fact, as shown in the Appendix, the limit $e_1 - e_3 = 0$ is covered by Eq. (12), and one finds $\delta k_{\mathrm{ST}} \equiv \delta k_c$.

Our theoretical considerations are confirmed by the representative numerical results for the critical voltage u_c and the critical wave number p_c of flexodomains, which are shown in Fig. 5 as function of $\delta k < 1$ for two different μ. In the case $\mu = 2$ the homogeneous Freedericksz state is replaced at $\delta k = \delta k_F(\mu = 2) \approx 0.206$ by the flexodomains; with increasing δk the critical voltage u_c monotonically decreases from $u_c = u_F$ on, while p_c increases from $p = 0$ on. For $\mu \to \infty$ (i.e., in the absence of flexoeffects) with $\delta k_F \to \delta k_{\mathrm{ST}}$ we get in the interval $\delta k_{\mathrm{ST}} \lesssim \delta k < 1$ the splay-twist Freedericksz distortion as a special case of the flexopatterns.

We will now return to the case $-1 < \delta k < \delta k_{\mathrm{low}} \approx -0.566$ in Fig. 4, where the exact $\mu_{\max}(\delta k)$ from Eq. (12) is slightly larger than $\bar{\mu}_{\max}(\delta k)$ given in Eq. (17). The reasoning, which led to the expression $\bar{\mu}_{\max}$, is rigorous as long as the p dependence of neutral curves is of the type shown in Fig. 3. As demonstrated for instance in Fig. 6 for $\delta k = -0.7$ this does not hold in the vicinity of $\delta k = -1$. The condition $u_0(p) = u_F$, which determines $\mu_{\max}(\delta k)$, is now already realized at a finite $p = p_c$, where $u_0(p)$ has a second local minimum of height $u_0(p_c) = u_F$. Since a merging of the two extrema is not required, as assumed in the calculation of $\bar{\mu}(\delta k)$ from Eq. (17), we have now $\mu_{\max}(\delta k) > \overline{\mu}_{\max}(\delta k)$ in agreement with Fig. 4. The exact neutral curve for $\delta k < \delta k_{\mathrm{low}}$ is only accessible by numerically solving Eq. (12). The special value $\delta k = \delta k_{\mathrm{low}}$,
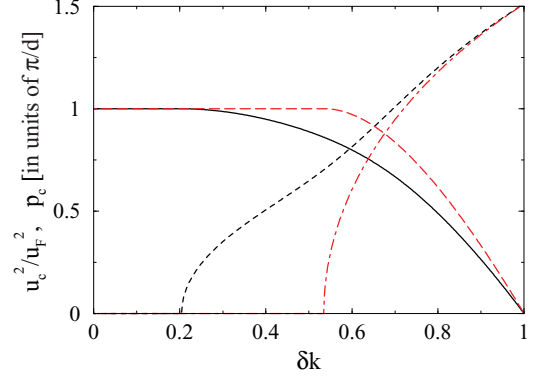
where $\mu_{\max}$ starts to deviate from $\mu_{\max}(\delta k)$, is obviously determined by the condition $\partial_p^2 u_0(p = 0) = \partial_p^4 u_0(p = 0) = 0$ at $u = u_F$ and $\mu = \mu_{\max}(\delta k)$. With the use of Eq. (12) one obtains from these conditions the following closed analytical expression for δk_{low}:

$$\delta k_{\mathrm{low}} = -\left[\frac{\pi^2(96 - 5\pi^2 - 8\sqrt{\pi^4 - 54\pi^2 + 468})}{-13\pi^4 + 832\pi^2 - 6912} \right]^{1/2}$$
$$= -0.5666, \qquad (20)$$

which agrees perfectly with the results presented in Fig. 4.

Finally we consider the case $\mu \propto \epsilon_a < 0$, where the dielectric torque is stabilizing and where the competing Freedericksz transition is absent. As already mentioned we found $\mu_{\min}(\delta k) \equiv \mu_{\min}^a(\delta k)$, given in Eq. (15). This can be explained by the fact, that exactly at $\mu = \mu_{\min}^a$ the purely imaginary roots $\pm i\lambda_2$ in Eq. (12) become real (see the Appendix). As a consequence the trigonometric functions $\sin(\lambda_2 \pi)$ and $\cos(\lambda_2 \pi)$ change into hyperbolic ones; then Eq. (12) allows only for the trivial solution $u = 0$, $p = 0$.
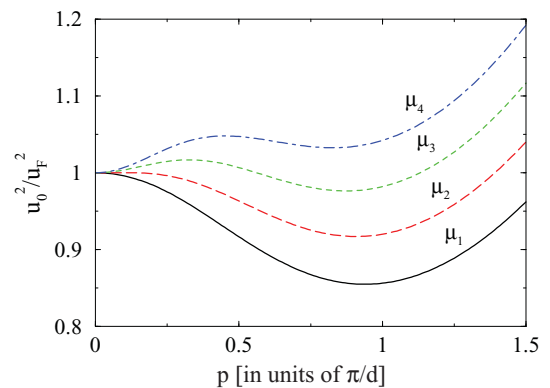

FIG. 6. (Color online) The neutral curve $u_0^2(p)$ as a function of p for $\delta k = -0.7$ and different μ where $\mu_1 = 0.11, \mu_2 = 0.12, \mu_3 = 0.13,$ and $\mu_4 = 0.14$.
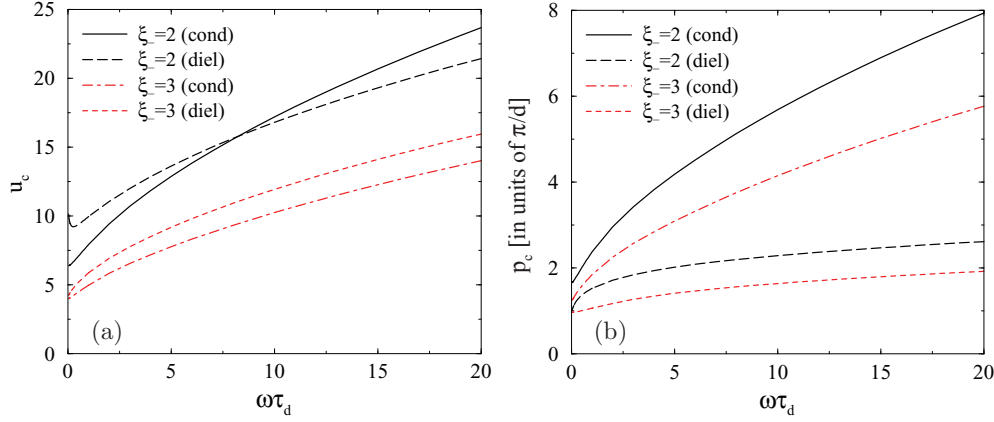
FIG. 7. (Color online) Critical voltage $u_c(\omega)$ in dimensionless units (a) and critical wave number (b) of the flexodomains as function of $\omega\tau_d$ for MBBA parameters with the flexostrengths $\xi_- = 2$ and $\xi_- = 3$. The symmetry of the solution is indicated.

B. Flexodomains driven by an ac voltage

While the onset of flexodomains in the presence of a dc voltage is well described by the closed expression [Eq. (12)], the case of an ac voltage requires in general numerical methods along the lines described in Sec. II. We consider only low frequencies ω where $\omega\tau_d < 20$, which corresponds to frequencies $f = \omega/(2\pi)$ up to 20 Hz for a cell of thickness $d = 10$ μm filled with MBBA. Note that we will sometimes use in the ac case instead of the voltage amplitude, $U_0 = E_0 d$, the *effective* [root mean square (RMS)] voltage $U_0/\sqrt{2}$, which derives from the time average of $U^2(t)$.

As a warm-up we first consider the Freedericksz transition ($\mu \propto \epsilon_a > 0$) at finite ω, where $\bar{n}_y \equiv 0$ and $p = 0$ in Eqs. (9). In analogy to Sec. III A we obtain the solution $\bar{n}_z(z,t) = \tilde{n}_z(t)\sin(z + \pi/2)$ with

$$\tilde{n}_z(t) = \tilde{n}_z(0)\exp\left\{-\int_0^t dt'[1 + \delta k - \mu u^2\cos^2(\omega t')]\right\}. \tag{21}$$

The solution $\tilde{n}_z(t)$ is periodic with period $T = 2\pi/\omega$ when the integral in Eq. (21) vanishes for the upper limit $t = T$. Thus the Freedericksz transition voltage, $u_{Fr}(\omega)$, for $\omega \neq 0$ is obtained as

$$[u_{Fr}(\omega)/\sqrt{2}]^2 = (1 + \delta k)/\mu = u_F^2. \tag{22}$$

Obviously it is the (nondimensionalized) *effective* (RMS) critical voltage $u_{Fr}(\omega)/\sqrt{2}$, which continuously approaches in the limit $\omega \to 0$ the Freedericksz transition voltage u_F [see Eq. (11)] in the dc case. At onset for $u = u_{Fr}$ the solution Eq. (21), normalized to its maximal value, has the following form:

$$\tilde{n}_z(t) = \exp\left[-(1 + \delta k)\frac{1 - \sin(2\omega t)}{2\omega}\right]. \tag{23}$$

At small ω Eq. (23) represents sudden burstlike director distortions similar to those shown in Fig. 9. The peaks of the $\tilde{n}_z(t)$ are located at $\omega t = \pi/4, 5\pi/4$, etc., and their width is proportional to $\sqrt{\omega}$.

Now we turn to the discussion of flexodomains where $n_y \neq 0$ and $p \neq 0$. The threshold u_c and the critical wave number p_c for finite frequency ω are calculated as explained

in Sec. II. As a rule we get two types of solutions, one with the conductive, the other with the dielectric temporal symmetry. In the following we use in general the material parameters of MBBA given in Eq. (3), where $k_{av} = 5.43$, $\delta k = 0.2265$ [see Eq. (7)] and $e_1 - e_3 = 1.34$. The dielectric torque is stabilizing, since $\epsilon_a = -0.53$. According to our investigations the existence of flexodomains in the dc case seems to be in general a necessary prerequisite for their existence in the ac case. In fact, at $\omega = 0$ flexodomains solutions do not exist for standard MBBA, since according to Eq. (10) we have $\mu = -1.6027 < \mu_{\min}(\delta k) = -0.815$; they have also not been observed in experiments. Thus we follow an idea in Ref. [20] and replace the difference $(e_1 - e_3)$ of the flexocoefficients in Eq. (9) by the product $\xi_- \cdot (e_1 - e_3)$ to study specifically the impact of the flexotorque. Flexodomains then exist for $\xi_- > 1.402$.

Representative examples for the dependence of the critical voltage u_c and the critical wave number p_c on the "flexostrength" ξ_- and on the ac frequency ω (in units of τ_d^{-1}) are shown in Fig. 7. For $\xi_- = 3$, corresponding to $\mu = -0.178$, the conductive symmetry prevails in the whole frequency range, while for $\xi_- = 2$, corresponding to $\mu = -0.401$, a switch over from the conductive symmetry to the dielectric symmetry takes place at larger $\omega\tau_d$. For both symmetry types the u_c and p_c curves rise monotonously as a function of $\omega\tau_d$ at fixed ξ_-. On the other hand, for the same symmetry type u_c and p_c are seen to decrease with increasing ξ_-, i.e., with growing magnitude of the flexotorque in analogy to the dc case.

To study the dependence of the critical voltage $u_c(\omega)$ and the critical wave number $p_c(\omega)$ on the elastic constants, MBBA parameters still have been used, except for a change of δk. Furthermore we have chosen $\xi_- = 2$ to favor the flexodomains against the homogeneous basic state. The resulting data are shown in Fig. 8. As before u_c and p_c increase monotonically with $\omega\tau_d$. We are, however, unable to offer a simple explanation for the change of symmetry with δk: While the dielectric symmetry of the flexodomains solutions prevails for $\delta k = -0.3, 0$, we find the conductive symmetry for $\delta k = 0.3$. The switch over between the symmetries happens at $\delta k \approx 0.1$.

In Fig. 9 we show an example of the director dynamics in the midplane ($z = 0$) as a function of time at the low frequency $\omega\tau_d = 0.05$. Remarkable are the sudden burstlike director
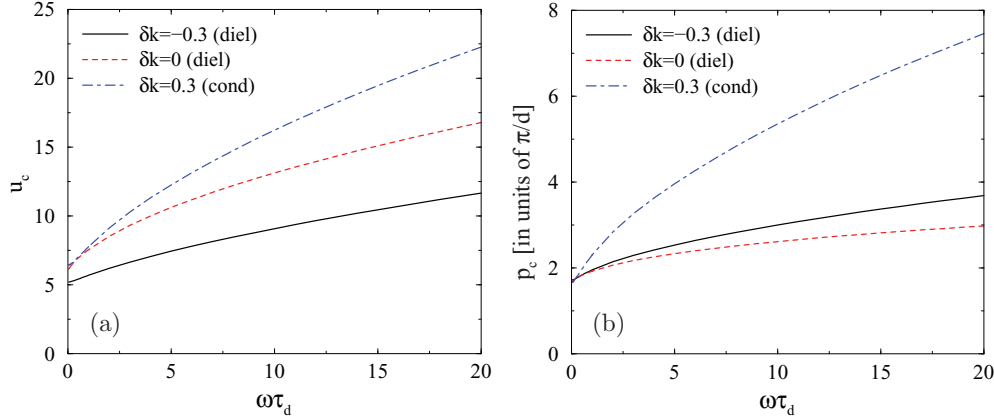
FIG. 8. (Color online) Critical voltage $u_c(\omega)$ in dimensionless units (a) and critical wave number (b) of the flexodomains as function of $\omega\tau_d$ for different δk and $\xi_- = 2$.

distortions; i.e., patterns would appear in the experiments only for very short time intervals. The conductive time symmetry for $\delta k = 0.3$ is reflected in the finite time average of $n_z(t)$; it vanishes for $n_y(t)$. On the other hand, for $\delta k < 0.1$ the behavior of n_z and n_y with the dielectric time symmetry would be just opposite.

Before we have concentrated on the MBBA-like materials with $\mu < 0$. In the case of $\mu > 0$ we are faced with the competition of flexodomains with the Freedericksz transition as discussed in Sec. III A for the dc case. The threshold voltage for the flexodomains increases monotonically with ω similar to the case of negative μ (see Figs. 7 and 8). Since, on the other hand, $u_{\mathrm{Fr}}(\omega)$ in Eq. (22) does not depend on ω, the Freedericksz transition will replace the flexodomains in any case above a certain finite ω. The frequency range where the flexodomains prevail will shrink with increasing μ.

1. The limit $\omega \to 0$

The limit $\omega \to 0$ is obviously not smooth: In the dc case both n_z and n_y have finite amplitudes at onset, while in the ac case the time average of one of the director components vanishes depending on the time symmetry. An interesting question is how this discontinuity is reflected in the critical
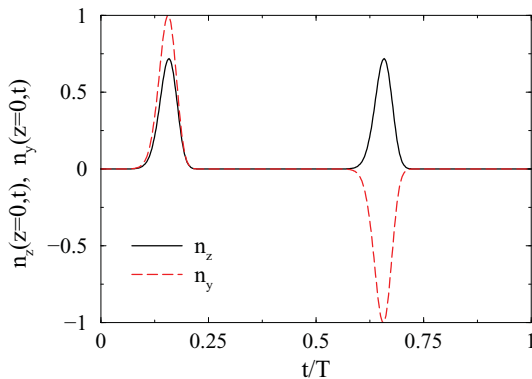

FIG. 9. (Color online) The director fields as a function of time at flexodomains threshold for a periodic excitation. $\omega\tau_d = 0.05$, $\delta k = 0.3$, and $\xi_- = 2$ (conductive symmetry).

voltage. As a rule of the thumb it is typically assumed, that the effective (RMS) voltages in the limit $\omega \to 0$ do not differ too much from critical voltages in the dc case. For the Freedericksz transition that difference is even zero [see Eq. (22)], and for electroconvection it is of the order of 10% of u_c (see the Appendix of Ref. [21]). In the case of flexodomains the corresponding differences are considerably larger in most cases.

As a representative example we discuss the $\omega \to 0$ limit of the u_c, p_c curves in Fig. 7 in comparison with the dc case from Eq. (12). Here MBBA material parameters have been used except that we allow for a modification of $e_1 - e_3$ via a factor ξ_- introduced above. At low frequencies the threshold curves both for $\xi_- = 2$ and $\xi_- = 3$ have conductive symmetry. For $\xi_- = 2$ ($\mu = -0.401$) we find for instance $u_{\mathrm{eff}}(0) \equiv u_c(\omega \to 0)/\sqrt{2} = 4.52$ compared to the dc value $u_c(0) = 3.49$; for $\xi_- = 3$ ($\mu = -0.178$) the difference between $u_{\mathrm{eff}}(0) = 2.83$ and $u_c(0) = 2.42$ is smaller. The discontinuity of $u_{\mathrm{eff}}(\omega)$ at $\omega = 0$ is associated with corresponding discontinuities of p_c: We find $p_c(\omega \to 0) = 1.66$ compared to $p_c(0) = 1.5$ for $\xi_- = 2$ and $p_c(\omega \to 0) = 1.25$ compared to $p_c(0) = 1.17$ when $\xi_- = 3$. For the parameters chosen in Fig. 8 we find comparable discontinuities as in Fig. 7 for $\xi_- = 2$, where the symmetry of the director configuration (dielectric for $\delta k = -0.3$, 0 and conductive for $\delta k = 0.3$) does not seem to play a significant role.

The discontinuities in the limit $\omega \to 0$ can be demonstrated most clearly in the special case $\delta k = 0$. Then the z dependence of the director fields in Eqs. (9) is rigorously described by the ansatz $\{\bar{n}_y(z,t), \bar{n}_z(z,t)\} = \{\hat{n}_y(t), \hat{n}_z(t)\} \sin(z + \pi/2)$. The transformation of the time variable $t \to t/\omega$ leads to

$$\omega\partial_t \hat{n}_y = -(p^2 + 1)\hat{n}_y + \mathrm{sgn}(e_1 - e_3)pu\cos(t)\hat{n}_z,$$
$$\omega\partial_t \hat{n}_z = -[p^2 + 1 - \mu u^2 \cos^2(t)]\hat{n}_z$$
$$+ \mathrm{sgn}(e_1 - e_3)pu\cos(t)\hat{n}_y. \quad (24)$$

From a mathematical point of view Eqs. (24) present an interesting dynamical system. It is kind of "singular" since the prefactor of the time derivatives is proportional to ω and
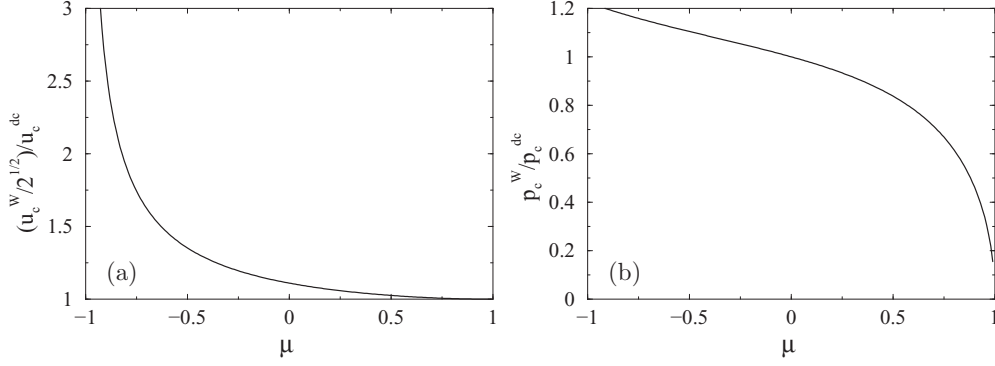
FIG. 10. The critical effective voltage for flexodomains $u_c^W/\sqrt{2}$ (a) and the critical wave number p_c^W (b) from Eq. (29) in the limit $\omega \to 0$ normalized to the dc values.

thus small in the limit $\omega \to 0$. For the special case $\mu = 0$ ($\epsilon_a = 0$) the general solution of Eqs. (24) is given as

$$\hat{n}_y(t) = \exp\left(-\frac{p^2+1}{\omega}t\right)\{c_1 e^{\phi(t)} - c_2 e^{-\phi(t)}\},$$

$$\hat{n}_z(t) = \exp\left(-\frac{p^2+1}{\omega}t\right)\{c_1 e^{\phi(t)} + c_2 e^{-\phi(t)}\}, \quad \text{with} \quad (25)$$

$$\phi(t) = \frac{\text{sgn}(e_1 - e_3)pu\sin(t)}{\omega},$$

where c_1, c_2 denote integration constants. Inspection of Eqs. (25) shows immediately that one is unable to find values of c_1, c_2 to allow for periodic solutions. This result is a further hint that the limit $\omega \to 0$ is not trivial, since in the dc case according to Eqs. (16) flexodomains do exist at $\mu \propto \epsilon_a = 0$.

The system Eqs. (24) for $\mu \neq 0$ has been in general investigated by the methods presented in Sec. II. To study in particular the limit $\omega \to 0$ we have employed the approximation scheme presented in the Appendix of Ref. [21], which is closely related to the familiar Wentzel-Kramers-Brillouin (WKB) approximation [22] in quantum mechanics. We use the ansatz $\{\hat{n}_y(t),\hat{n}_z(t)\} = \{\tilde{n}_y(t),\tilde{n}_z(t)\} \exp[S_0(t)/\omega]$ and neglect the derivatives of $\tilde{n}_y(t)$, $\tilde{n}_z(t)$. The resulting coupled homogeneous equations for $\tilde{n}_y(t)$, $\tilde{n}_z(t)$ will have a nontrivial solution when the corresponding determinant vanishes. In this way the following equation for $S_0(t)$ is obtained:

$$(\partial_t S_0)^2 + g_1(t)\partial_t S_0 + g_0(t) = 0, \quad (26)$$

where

$$g_1(t) = 2(p^2+1) - \mu u^2 \cos^2(t),$$
$$g_0(t) = (p^2+1)^2 - [p^2 + \mu(p^2+1)]u^2 \cos^2(t). \quad (27)$$

From Eq. (26) we obtain

$$2\partial_t S_0 = -g_1 + \sqrt{g_1^2 - 4g_0}. \quad (28)$$

In analogy to the discussion of the Freedericksz transition [see Eq. (21)] the solution is bounded when the average over one period (2π) of the right-hand side of Eq. (28) vanishes. The required time integration can be performed analytically and

leads to the following implicit equation for the neutral curve $u_0(p) \equiv u_0(p,\omega \to 0)$:

$$\pi\left[2(p^2+1) - \mu u_0^2/2\right]|\mu|$$
$$= 2\sqrt{p^2\mu^2 u_0^2} + \left(4p^2 + \mu^2 u_0^2\right)\arcsin\left(\sqrt{\frac{\mu^2 u_0^2}{4p^2 + \mu^2 u_0^2}}\right). \quad (29)$$

This transcendental equation is solved numerically, which yields within the WKB approximation the critical voltage u_c^W and the critical wave number p_c^W of the flexodomains in the limit $\omega \to 0$. The data agree perfectly with the exact solution of Eq. (24) on the basis of the monodromy matrix method in the limit $\omega \to 0$. In Fig. 10(a) the ratio of dimensionless effective (RMS) critical voltage ($u_c^W/\sqrt{2}$), and the dc value is plotted as function of μ. While this ratio is near 1 for $-1/2 < \mu < 1$, it increases strongly when further decreasing μ toward $\mu = \mu_{\min}(\delta k = 0) = -1$. The corresponding ratio of the critical wave number p_c^W and the dc value is shown in Fig. 10(b). In comparison to the critical voltages one finds even larger deviations of this ratio from one in particular at larger positive μ where p_c itself becomes small.

Finally we would like to point out that the transition to the dc limit and the interesting time evolution of director perturbations characterized by bursts depend also on the wave-form of the exciting ac voltage. To demonstrate this we have considered a square-wave excitation that consists of an alternating sequence of constant voltages $\pm u$ on time intervals of the length $T/2$, i.e., $U(t) = U_0\text{sgn}[\cos(\omega t)]$. Then Eqs. (9) can be solved quasianalytically by joining continuously the analytical solutions on the parts with constant voltage, which leads to an implicit transcendental equation ("boundary determinant") for the neutral curve $u_0(p)$. Since for small $\omega\tau_d$ the values of u_c and p_c are practically determined by the long-time intervals of constant u, they are practically identical to the dc values. Consequently, as demonstrated in Fig. 11, the time variations of n_z, n_y are rather smooth compared to the bursts observed with the harmonic ac driving at low ω.

In the following section, we will study the alternative electroconvection (EC) solutions of the nematohydrodynamic equations, which compete with the flexodomains. In general it will turn out that only for small ω the flexodomains have the chance to prevail.
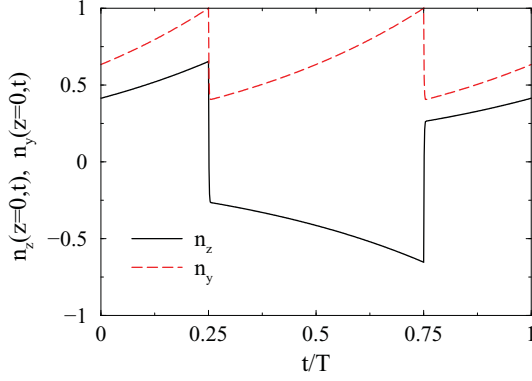
FIG. 11. (Color online) The director fields as function of time at the threshold of flexodomains for a square-wave excitation. $\omega\tau_d = 0.05$, $\delta k = 0$, and $\xi_- = 2$ (dielectric symmetry).

IV. ELECTROCONVECTION

The salient elements of the positive feedback loop leading to the dissipative electro-hydrodynamic instability (EC), which are contained in the familiar nematohydrodynamic equations (see Sec. II), have been elucidated by Carr and Helfrich [12,13]: A necessary condition is that the nematic is "contaminated" by a small amount of mobile ions, which results in a finite, though very small, electrical conductivity of the order of $\sigma_0 = 10^{-8}$ $(\Omega$ m$)^{-1}$. Then spatial fluctuations of

n in the presence of a nonzero E lead to an electric charge density $\rho_{el} = \nabla \cdot D + \rho_{fl}$. The first contribution to ρ_{el} is the standard one, which derives from the dielectric displacement $D = \epsilon_0 \epsilon E$. The latter "nonstandard" contribution, the flexocharge ρ_{fl}, is determined by the earlier introduced flexopolarization as $\rho_{fl} = \nabla \cdot P_{fl}$. Via the Coulomb force, $\rho_{el}E$, in the (generalized) Navier-Stokes equation a material flow, v, is driven which exerts an additional viscous torque on the director. Under a favorable constellation of the material parameters the viscous torque reinforces the initial director distortion leading to EC. For more details in particular a very recent review [14] might be useful, where systematically the sensitive influence of the sign of the dielectric anisotropy ϵ_a, of the electric conductivity, σ_a, and of the basic director configuration on the patterns is discussed.

Exploiting the calculational scheme briefly discussed in Sec. II we have precisely characterized the onset of EC. While in flexodomains the time scale is set by the director relaxation time $\tau_d \propto d^2$ [see Eq. (10)], in electroconvection the thickness independent charge relaxation time $\tau_q = \epsilon_0\epsilon_\perp/\sigma_\perp$ plays an important role as well. Thus we observe in EC a thickness dependence of the critical properties, which cannot be absorbed by a suitable frequency rescaling. For definiteness we concentrate in the following on a nematic layer of thickness $d = 10$ μm and use MBBA parameters (if not otherwise stated), where $\tau_d = 0.2$ s and $\tau_q = 4.65 \times 10^{-3}$ s. The impact of the flexocharge ρ_{fl} on EC is determined by the sum $(e_1 + e_3)$
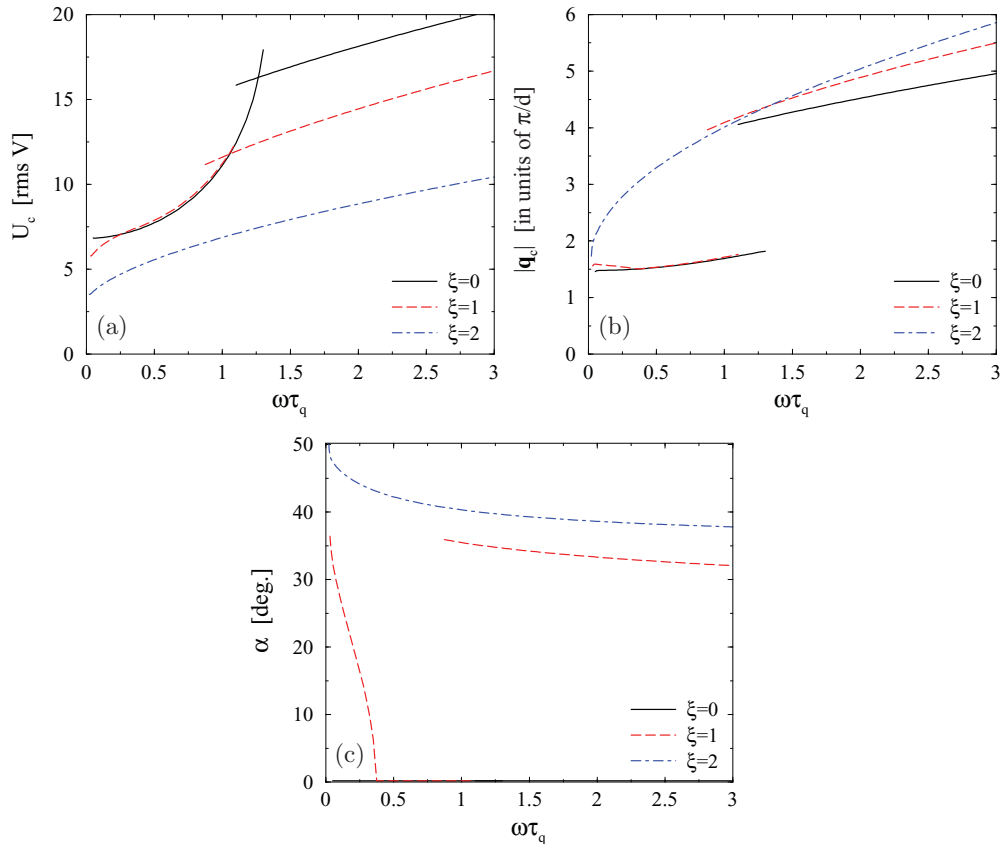

FIG. 12. (Color online) Critical effective voltage U_c of electroconvection (RMS value in volts) (a), modulus of the critical wave vector $|\mathbf{q}_c|$ (b), and the angle α of the critical wave vector with the x axis (c) as a function of frequency ω (in units of the charge relaxation time τ_q) for different magnitudes of the flexocoefficients $\xi = \xi_- = \xi_+$ (for more details, see text).
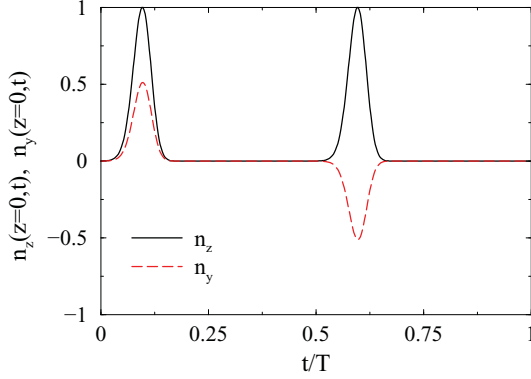
FIG. 13. (Color online) The director fields as a function of time at EC threshold for $\omega\tau_q = 2.3 \times 10^{-3}$ ($\omega\tau_d = 0.1$).

of the flexocoefficients. In analogy to the factor ξ_- introduced in Sec. (9) to tune the strength of the flexotorque, we replace here in addition $(e_1 + e_3)$ by $\xi_+(e_1 + e_3)$ to allow for a selective modification of ρ_{fl}. To facilitate a direct comparison with experiments we will refer to effective (RMS) critical voltages in physical units in this section.

In Fig. 12 we present representative critical EC data for MBBA parameters [16] as a function of $\omega\tau_q$ for different $\xi = \xi_- = \xi_+$. In general U_c and $|\boldsymbol{q}_c|$ [see Figs. 12(a), and 12(b)] increase monotonically with increasing ω. While the two curves are smooth for $\xi = \xi_- = \xi_+ = 2$, where the dielectric symmetry prevails, we observe discontinuities for the two smaller ξ. Here the conductive branch at small ω is replaced by the dielectric one at a crossover frequency ω_c where $\omega_c\tau_q \approx 1.2$. The obliqueness of the rolls, as shown in Fig. 12(c), is measured by the angle α between $\boldsymbol{q}_c$ and the preferred director orientation in the basic planar configuration (our x axis). In the absence of flexoeffects ($\xi = 0$) we find $\alpha \equiv 0$ for all ω. When $\xi_- = \xi_+ = 1$ the obliqueness of the rolls in the conductive regime vanishes continuously at the "Lifshitz point" $\omega_L\tau_q \approx 0.35$ and becomes finite again in the dielectric regime. At the largest $\xi = 2$ the angle $\alpha \approx 40°$ is finite for all ω. Note that recently for other nematic material a "Lifshitz point" in the dielectric regime of EC has been identified as well [9].

In analogy to the flexodomains the limit $\omega \to 0$ for the critical voltage in EC is not smooth. However, the dc-critical voltage is much better approximated by the limit $\omega \to 0$ of the effective voltage $U_c(\omega)$ than for the flexodomains. This finding can be explained within a WKB approximation [21], where the relative corrections are indeed small, on the order of τ_q/τ_d (up to some q-dependent factors). EC shares, however, with the flexodomains the typical spiky time evolution of the director components at very low ω, as comparison of Fig. 9 with Fig. 13 shows.

Besides the flexocoefficients a further crucial parameter is the anisotropy σ_a of the electric conductivity, since the Carr-Helfrich charge separation mechanism depends strongly on the magnitude and the sign of $\sigma_a/\sigma_\perp$. This dependence had not been investigated in detail for many years, since in the materials used at that time $\sigma_a/\sigma_\perp$ would vary only between 0.3 and 0.7. Recently, however, materials have been found, where by decreasing the temperature σ_a decreases as well;
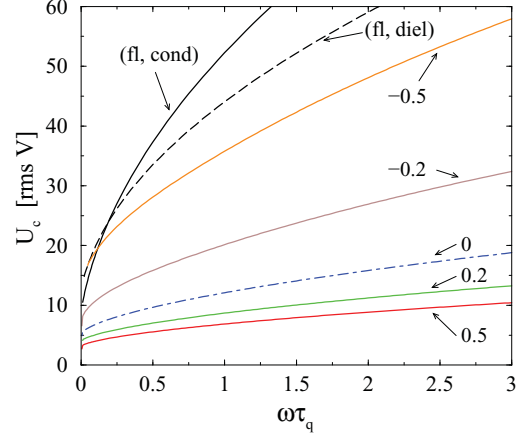

FIG. 14. (Color online) Critical voltage U_c (RMS value in volts) for EC as a function of frequency ω (in units of the charge relaxation time τ_q) for five different values of $\sigma_a/\sigma_\perp$ between 0.5 and -0.5 and for $\xi_- = \xi_+ = 2$. The corresponding critical voltages for the flexodomains (conductive symmetry at small ω and dielectric symmetry at larger ω) are included as well.

it passes even zero and becomes negative. Thus it has now become important and attractive to study the σ_a dependence in more detail. This has been done partially in Ref. [15], where $U_c(\omega)$ has been observed to move up in general with decreasing σ_a. To study the details we have taken MBBA parameters as before except that $\sigma_a/\sigma_\perp$ was allowed to vary. Furthermore, to explore the competition with flexodomains, which do not exist for standard MBBA (see Sec. III B), the flexocoefficients have to be increased as well. We have centered on the case $\xi = \xi_- = \xi_+ = 2$, which has been shown already in Fig. 12 for EC and in Fig. 7 for flexodomains. The EC threshold, which is characterized by the dielectric symmetry, increases strongly with decreasing $\sigma_a/\sigma_\perp$ for all ω as documented in Fig. 14. Only for $\sigma_a/\sigma_\perp = -0.5$ and for very small frequencies up to $\omega\tau_q \approx 0.1$ (where $\omega\tau_d \approx 3.6$) do flexodomains with conductive symmetry prevail. For the case $\xi_- = \xi_+ = 1$ one finds the same behavior of $U_c(\omega)$ when changing σ_a, while the flexodomains do not exist.
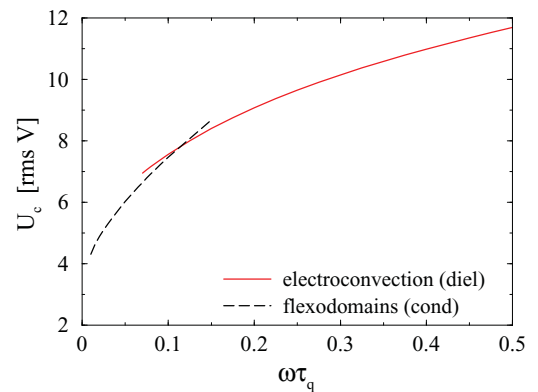

FIG. 15. (Color online) Critical effective voltage U_c (RMS value in volts) as a function of frequency ω (in units of the charge relaxation time τ_q) for flexodomains and EC patterns. Material parameters of MBBA except $\sigma_a/\sigma_\perp = 0.2$, $\xi_- = 3$, and $\xi_+ = 0.25$.
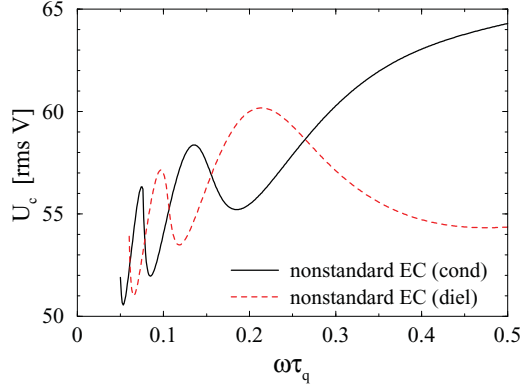
FIG. 16. (Color online) Critical effective voltage U_c of electro-convection (RMS value in volts) as a function of frequency ω (in units of the charge relaxation time τ_q) for MBBA material parameters ($\xi_+ = \xi_- = 1$) except $\sigma_a/\sigma_\perp = -0.05$.

To find material combinations, where flexodomains have a chance to dominate the pattern-forming instability for standard and not too small values of σ_a, one has obviously to choose different values of ξ_- and ξ_+. One needs a relatively large ξ_- to increase the flexotorques, which are responsible for the existence of flexodomains. Conversely, ξ_+ should be fairly small to suppress the positive influence of the flexocharge on EC. Since systematic experimental studies, also including different nematic materials, are lacking so far, extended parameter studies seem to be futile at the moment. So we present only one example with $\xi_- = 3$, $\xi_+ = 0.25$, and $\sigma_a/\sigma_\perp = 0.2$, where flexodomains (with conductive symmetry) indeed prevail EC at low frequencies as shown in Fig. 15.

Finally, we address briefly the intriguing limiting behavior of EC at low frequencies, when ξ_- is too small for the existence of flexodomains at $\omega = 0$. As demonstrated in Fig. 16, we predict in this situation a persistent switching between the conductive and the dielectric solutions for $\sigma_a/\sigma_\perp = -0.05$.

V. CONCLUSIONS

In this paper we have investigated pattern-forming instabilities in nematic liquid crystals originally in the basic planar configuration, which are driven out of equilibrium by an electric dc or ac voltage applied perpendicular to the layer. In the basic state the director field is homogeneous over the nematic layer, and a preferred direction is singled out in the layer plane.

In particular we have concentrated on the impact of the flexoeffects, which generically exist, when the director varies in space. They result, on the one hand, in the flexotorque, which may lead at sufficiently large voltage amplitude to the flexodomains. These are spatially periodic in the layer plane and can be visualized in experiments as stripes parallel to the preferred planar direction. In this paper the bifurcation scenario to flexodomains is for the first time comprehensively analyzed for applied dc and ac voltages. We have also demonstrated that the well-established splay-twist Freedericksz transition in the absence of flexoeffects can be described in this framework. Particular focus was on the intriguing phenomena in the limit of the vanishing ac frequency ω of

the driving voltage. One finds, for instance, periodic-in-time, burstlike excursion of the director from the planar basic state.

Furthermore we have investigated the competition between the flexodomains and the familiar EC convective rolls. The latter are visualized as stripes, which include a finite angle typically larger than 45° with the preferred axis. In general EC prevails, except at very low frequencies where the flexodomains may trigger the destabilization of the homogeneous basic state. Like the flexodomains the EC pattern appears also periodically in time as sudden bursts, while the system remains otherwise in the structureless basic planar state.

We expect that our theoretical analysis will motivate further investigations of electrically driven pattern formation in nematics with special focus on the low-frequency regime. Though in particular the sudden, periodic-in-time "blow-up" of flexodomains and EC patterns as well a crossover between them have been clearly seen in recent experiments [9], a quantitative comparison with the theory is far from trivial. On one hand, one is faced with considerable uncertainties in the material parameters even for a nematic like MBBA. Moreover, one has to realize that the nematic layer is confined by metal-lically coated glass plates with a thin polymeric alignment film on top, which themselves may have fairly complicated electric properties. Thus the whole system is represented as an equivalent circuit diagram (see, e.g., Refs. [23,24]) where the total voltage applied to the cell is different from "theoretical" results like U_c, which represent only the voltage drop over the nematic layer. The necessary corrections to U_c are not easy to model and would also require systematic measurements on the empty cell. Finally the coexistence between flexodomains and EC pattern in the nonlinear regime when their linear thresholds are comparable has to be investigated. For instance, such a scenario has indeed been observed in hybrid aligned nematic cells [25] in the presence of a dc voltage.

APPENDIX: FLEXODOMAINS DRIVEN BY A DC VOLTAGE

In this Appendix we describe briefly the derivation of the implicit equation (12), which yields the neutral curve $u_0(p)$. We use the ansatz $\{\bar{n}_z(z), \bar{n}_y(z)\} = \{\hat{n}_z, \hat{n}_y\}e^{\lambda z}$ in Eq. (9) and set $\sigma = 0$ from the beginning. Thus we arrive at a linear homogeneous 2×2 system for $\hat{n}_y$ $\hat{n}_z$, which leads to the following secular equation for λ:

$$[p^2(1 + \delta k) - (1 - \delta k)\lambda^2][p^2(1 - \delta k) - \mu u^2 - (1 + \delta k)\lambda^2]$$
$$- p^2[\text{sgn}^2(e_1 - e_3)u^2 - 4\delta k^2\lambda^2] = 0. \tag{A1}$$

From Eq. (A1) we obtain the two eigenvalues $\lambda^2 = \lambda_1^2, -\lambda_2^2$, where $\lambda_1^2, \lambda_2^2 > 0$, which read as follows:

$$\lambda_1^2 = p^2 - \frac{\mu u^2}{2(1 + \delta k)} + S, \quad \lambda_2^2 = -p^2 + \frac{\mu u^2}{2(1 + \delta k)} + S,$$

$$S = \left\{ \frac{\text{sgn}^2(e_1 - e_3) + 2\delta k\mu}{1 - \delta k^2} p^2 u^2 + \left[\frac{\mu u^2}{2(1 + \delta k)} \right]^2 \right\}^{1/2}. \tag{A2}$$

The eigenvector of the linear system is chosen as

$$\{\hat{n}_z(\lambda), \hat{n}_y(\lambda)\} = \left\{ 1, p \frac{\text{sgn}(e_1 - e_3)u - 2\delta k\lambda}{p^2(1 + \delta k) - (1 - \delta k)\lambda^2} \right\}. \quad \text{(A3)}$$

In line with the standard procedure we express the general solution as a linear combination of the eigenmodes (A3)

$$\bar{n}_z(z) = a_1 e^{\lambda_1 z} + a_2 e^{-\lambda_1 z} + a_3 e^{i\lambda_2 z} + a_4 e^{-i\lambda_2 z},$$
$$\bar{n}_y(z) = a_1 \hat{n}_y(\lambda_1)e^{\lambda_1 z} + a_2 \hat{n}_y(-\lambda_1)e^{-\lambda_1 z}$$
$$+ a_3 \hat{n}_y(i\lambda_2)e^{i\lambda_2 z} + a_4 \hat{n}_y(-i\lambda_2)e^{-i\lambda_2 z}, \quad \text{(A4)}$$

to fulfill the boundary conditions $\bar{n}_z(\pm\pi/2) = \bar{n}_y(\pm\pi/2) = 0$. A nontrivial solution exists, when the determinant of the resulting set of four linear homogeneous equations for the a_i vanishes. The resulting implicit equation for the neutral curve has been already given in Eq. (12). It contains the λ_i (A2) and coefficients A_i, which are given as follows:

$$A_1 = \left[\left(f_1^2 \lambda_2^2 - f_2^2 \lambda_1^2 \right) C^2 + \left(\lambda_1^2 + \lambda_2^2 \right)^2 D^2 \right],$$
$$A_2 = 2 f_1 f_2 C^2, \quad \text{(A5)}$$

with

$$f_1 = \lambda_1^2 - B, \quad f_2 = \lambda_2^2 + B, \quad B = p^2 \frac{1 + \delta k}{1 - \delta k},$$
$$C = \frac{2\delta k}{\sqrt{1 - \delta k^2}}, \quad D = \frac{\text{sgn}(e_1 - e_3)u}{\sqrt{1 - \delta k^2}}. \quad \text{(A6)}$$

MAPLE and MATHEMATICA have been very useful in performing and in validating all our calculations.

The Freedericksz transition in the absence of flexoeffects ($e_1 - e_3 = 0$) is formally covered by Eq. (12) as well. First, the voltage u appears always in the combination (μu^2) where according to Eq. (10) the factors ($e_1 - e_3$) cancel. Furthermore we have $D \equiv 0$ [see Eq. (A6)] in this limit. The critical value δk_{ST} at which the splay-twist Freedericksz transition starts to prevail is obviously determined by the conditions $\partial_p^2 u_0(p = 0) = \partial_p^4 u_0(p = 0) = 0$ at $u_0(p)/u_F = 1$. This condition is exploited by expanding Eq. (12) to order p^4, and we arrive in fact at an expression for δk_{ST}, which is identical to δk_c in Eq. (19). Note that in Ref. [4] instead of an exact value for $\delta k_c = 0.534624$ the approximation $\delta k_c \approx 0.53$ was given.

On the background of the exact textbook analysis presented in this Appendix it is easy to demonstrate why the authors of Refs. [10,11] arrived at wrong results. Starting from the basic equations for the flexodomains in the dc case [equivalent to Eqs. (9)] at first a set of two coupled ODEs that contain only second-order z derivatives has been obtained [see Eq. (12) in Ref. [11]]. Unfortunately the second step, namely, diagonalizing the ODEs by a "unitary" transformation $\hat{V}$ [see Eq. (14) in Ref. [11]], does not work since $\hat{V}$ explicitly depends on z. Thus the main conclusion in Ref. [11] that the eigenmodes associated with the eigenvalues P and Q [see Eq. (20) in Ref. [11]] would decouple is untenable. This applies also to the resulting simple relation $\tan(iQd) = 0$ [see Eq. (22) in Ref. [11]], which would replace our correct Eq. (12) for the neutral curve $u_0(p)$. Note that the same erroneous procedure has appeared already in a previous investigation [26], cited also in Refs. [10,11].

[1] P. G. de Gennes and J. Prost, *The Physics of Liquid Crystals* (Clarendon Press, Oxford, 1993).

[2] S. Chandrasekhar, *Liquid Crystals* (Cambridge University Press, Cambridge, UK 1992).

[3] Á. Buka and L. Kramer, editors, *Pattern Formation in Liquid Crystals* (Springer-Verlag, New York, 1996).

[4] F. Lonberg and R. B. Meyer, Phys. Rev. Lett. **55**, 718 (1985).

[5] A. Buka and L. Kramer, J. Phys. II (France) **2**, 315 (1992); Phys. Rev. A **45**, 5624 (1992).

[6] Yu. P. Bobylev and S. A. Pikin, Zh. Eksp. Teor. Fiz. **72**, 369 (1977) [Sov. Phys. JETP **45**, 195 (1977)].

[7] M. I. Barnik, L. M. Blinov, A. N. Trufanov, and B. A. Umanskii, Zh. Eksp. Teor. Fiz. **73**, 1936 (1977) [Sov. Phys. JETP **46**, 1016 (1977)].

[8] M. I. Barnik, L. M. Blinov, A. N. Trufanov, and B. A. Umanski, J. Phys. (France) **39**, 417 (1978).

[9] M. May, W. Schöpf, I. Rehberg, A. Krekhov, and Á. Buka, Phys. Rev. E **78**, 046215 (2008).

[10] H. P. Hinov and Y. Marinov, Mol. Cryst. Liq. Cryst. **503**, 45 (2009).

[11] Y. G. Marinov and H. P. Hinov, Eur. Phys. J. E **31**, 179 (2010).

[12] E. F. Carr, Mol. Cryst. Liq. Cryst. **7**, 253 (1969).

[13] W. Helfrich, J. Chem. Phys. **51**, 4092 (1969).

[14] Á. Buka, N. Éber, W. Pesch, and L. Kramer, in *Self-Assembly, Pattern Formation and Growth Phenomena in Nano-Systems*, edited by A. A. Golovin and A. A. Nepomnyashchy (Springer, Dordrecht, 2006), p. 55.

[15] A. Krekhov, W. Pesch, N. Éber, T. Tóth-Katona, and Á. Buka, Phys. Rev. E **77**, 021705 (2008).

[16] The flexocoefficients e_1, e_2 for MBBA are taken from Ref. [20]. The other material parameters can be found, for instance, as the set MBBA I in the Appendix of Ref. [21].

[17] J. K. Hale, *Ordinary Differential Equations* (Wiley, New York, 1969).

[18] J. Heuer, T. John, and R. Stannarius, Phys. Rev. E **78**, 036218 (2008).

[19] J. Stelzer, M. A. Bates, L. Longa, and G. R. Luckhurst, J. Chem. Phys. **107**, 7483 (1997).

[20] W. Thom, W. Zimmermann, and L. Kramer, Liq. Cryst. **4**, 309 (1989).

[21] E. Bodenschatz, W. Zimmermann, and L. Kramer, J. Phys. (France) **49**, 1875 (1988).

[22] C. M. Bender and S. A. Orszag, *Advanced Mathematical Methods for Scientists and Engineers* (McGraw Hill, New York, 1978).

[23] M. Oh-e, K. Kondo, and Y. Kando, Liq. Cryst. **17**, 95 (1994).

[24] H. Seiberle and M. Schadt, Mol. Cryst. Liq. Cryst. **239**, 229 (1994).

[25] V. A. Delev, A. P. Krekhov, and L. Kramer, Mol. Cryst. Liq. Cryst. **366**, 849 (2001).

[26] V. P. Romanov and G. K. Sklyarenko, Zh. Eks. Teor. Fiz. **112**, 1675 (1997) [JETP **85**, 914 (1997)].